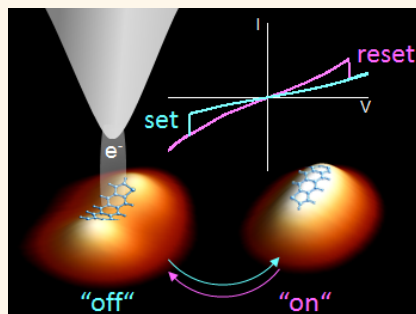


Bipolar Conductance Switching of Single Anthradithiophene Molecules

Bogdana Borca,^{*,†,‡,∞} Verena Schendel,^{†,‡} Rémi Pétuya,[‡] Ivan Pentegov,[†] Tomasz Michnowicz,[†] Ulrike Kraft,[†] Hagen Klauk,[†] Andrés Arnau,^{§,‡} Peter Wahl,^{†,||} Uta Schlickum,^{*,†} and Klaus Kern^{†,‡}

[†]Max-Planck-Institute for Solid State Research, 70569 Stuttgart, Germany, [‡]Donostia International Physics Centre, E-20018 Donostia - San Sebastián, Spain, [§]Departamento de Física de Materiales UPV/EHU and Material Physics Center (MPC), Centro Mixto CSIC-UPV/EHU, E-20018 Donostia - San Sebastián, Spain, ^{||}SUPA, School of Physics and Astronomy, University of St Andrews, North Haugh, St Andrews, KY16 9SS, United Kingdom, and [#]Institut de Physique de la Matière Condensée, École Polytechnique Fédérale de Lausanne (EPFL), CH-1015 Lausanne, Switzerland. [∞]B. Borca and V. Schendel contributed equally. ^{∞∞}Present address: National Institute of Materials Physics, Atomistilor 105b, 077125 Magurele-Ilfov, Romania.

ABSTRACT Single molecular switches are basic device elements in organic electronics. The pentacene analogue anthradithiophene (ADT) shows a fully reversible binary switching between different adsorption conformations on a metallic surface accompanied by a charge transfer. These transitions are activated locally in single molecules in a low-temperature scanning tunneling microscope. The switching induces changes between bistable orbital structures and energy level alignment at the interface. The most stable geometry, the “off” state, which all molecules adopt upon evaporation, corresponds to a short adsorption distance at which the electronic interactions of the acene rings bend the central part of the molecule toward the surface accompanied by a significant charge transfer from the metallic surface to the ADT molecules. This leads to a shift of the lowest unoccupied molecular orbital down to the Fermi level (E_F). In the “on” state the molecule has a flat geometry at a larger distance from the surface; consequently the interaction is weaker, resulting in a negligible charge transfer with an orbital structure resembling the highest occupied molecular orbital when imaged close to E_F . The potential barrier between these two states can be overcome reversibly by injecting charge carriers locally into individual molecules. Voltage-controlled current traces show a hysteresis characteristic of a bipolar switching behavior. The interpretation is supported by first-principles calculations.



KEYWORDS: *cis/trans* ADT isomers · Cu(111) · STM · DFT · conformational and electronic switching

A visionary perspective of molecular electronics is the use of single molecules as functional entities in electronic devices.¹ In this context, important components are molecular switches,^{2,3} which can be interconverted reversibly between two or more stable states. Scanning tunneling microscopy and spectroscopy (STM/STS) represents an ideal tool to characterize and manipulate single atoms and molecules on surfaces.⁴ Several switching mechanisms have been explored previously with molecular and submolecular resolution and have been induced locally by tunneling electrons,^{5–23} by an applied electric field,^{24,25} or by combined stimuli^{26–28} in the STM tunnel junction. Changes of the molecular configurations were identified as changes of the folding in complex organic molecules,⁵ different types of isomerization processes,^{7,13,15,18–24,28} changes of the atomic position in metal–organic complexes,^{6,26} and formation and dissociation of chemical

bonds.^{8–11,16,17,25} These conformational changes may be accompanied by charging and discharging processes.^{12–16,27,28} Recently, another scenario was proposed theoretically in which a switching process of an individual molecule is related to bistable electronic states. These are associated with different bonding strengths and hybridization degrees of the molecules to a metallic substrate, resulting in a change of the bending of the molecular conformation concomitant with a change of the adsorption distance.²⁹

In this study, we focus on single molecular switches consisting of individual anthradithiophene (ADT) molecules. ADT is a structural analogue of pentacene, with two sulfur-containing groups at each molecular terminal side representing *cis*- and *trans*-diastereomers.³⁰ The switching of individual molecules is activated locally by injecting charge carriers from the STM tip apex into the molecule. The molecules

* Address correspondence to bogdana.borca@infim.ro, u.schlickum@fkf.mpg.de.

Received for review September 25, 2015 and accepted November 18, 2015.

Published online November 18, 2015
10.1021/acsnano.5b06000

© 2015 American Chemical Society

are reversibly interconverted by voltage pulses of opposite polarity between two different adsorption geometries that correspond to two different electronic conformations of the molecule. The characteristic parameter responsible for the structural and electronic changes is the adsorption distance that determines the bonding strength and the degree of hybridization between the ADT molecule and the surface, similar to the recently proposed case of benzene derivatives.²⁹ Our first-principles calculations using van der Waals density functionals where exchange and correlation are treated consistently (vdW-DF-cx)^{31,32} allow us to propose a model based on the appearance of two adsorption states corresponding to two different geometric (bent and planar) and electronic conformations. These two conformations are induced by two main driving forces, the S–Cu bond length and the adsorption constraint for an optimal binding of the acene groups to the substrate, similar to pentacene.^{33,34}

RESULTS AND DISCUSSION

Individual ADT molecules deposited at 200 K on the Cu(111) surface adsorb with their long axis along the high-symmetry directions of the substrate, where *cis*- and *trans*-isomers adopt the same adsorption conformation (Figure 1a). In topographic images acquired with a metallic tip the two isomers are practically indistinguishable and all molecules appear in a “dumbbell-like” shape. By functionalizing the STM tip with a single ADT molecule (by picking up the encircled molecule in Figure 1a) the orbital structure can be resolved (Figure 1b) and thus the *cis*- and *trans*-diastereomers can be identified. Different configuration characteristics for each isomer at the molecular extremities, with higher charge density on the same side (*cis*) or on the opposite side (*trans*), are observed, as indicated by the arrows in Figure 1c,d.

On placing the tip above the center of the molecules, as shown in Figure 2a,b, a negative voltage pulse of -0.5 V was applied. During this measurement the feedback loop was opened and the tunneling current recorded. After a certain time, an abrupt change in the tunneling current, *i.e.*, a step-like (for *cis*-ADT) and a double step-like (for *trans*-ADT) behavior, is observed (Figure 2c,d). Rescanning the same molecules reveals that the increase in the current is associated with a change in the topographic appearance (Figure 2a,b). In addition, in the switched conformation the *trans*-ADT molecule is rotated by about 10° (Figure 2b), which can be related to the double-step feature in the current trace (Figure 2d). Switching the molecule back to the initial adsorption conformation is induced by a positive voltage (Figure 2c,d lower panel). In the following, we will refer to the initial adsorption conformation as the “off” state and the conformation related to a higher conductance (in open feedback-loop conditions) as the “on” state.

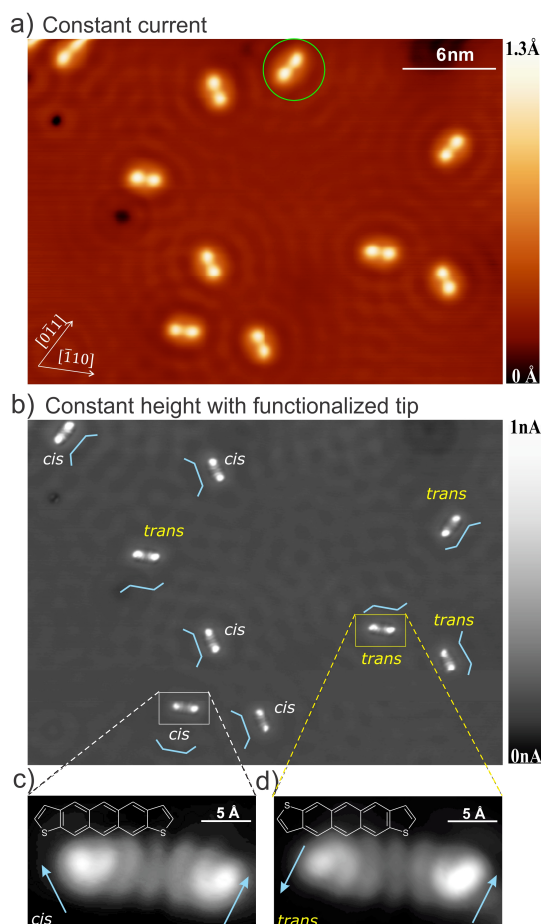


Figure 1. (a) 30×20 nm² STM topography acquired in constant current mode ($I = 100$ pA, $V = 100$ mV). The encircled molecule was used to functionalize the tip by vertical manipulation. (b) Isomer-resolved STM image obtained with the functionalized tip of the same area as (a) at constant height ($V = 5$ mV). Guiding lines are drawn for each molecular configuration. (c, d) Enlarged high resolution images of the two ADT molecules framed in (b), representing the *cis*-ADT and *trans*-ADT isomers. Guiding arrows are drawn at the molecular extremities.

The measurements suggest that the two different adsorption conformations of ADT molecules rely on the interplay between the S-containing groups and the acene group position with respect to the Cu substrate atoms. In Figure 2a,b (upper panels) ball-and-stick models for both adsorption conformations on Cu(111) are represented in a top view for both isomers. The acene group tends to have the benzene units centered over the hollow sites of the surface, which favors alignment of the molecules along the high-symmetry directions as in the case of pentacene on Cu(111).³⁵ In addition, there is a tendency of the S atoms of the thiophene rings to sit on top of Cu atom positions.³⁶ The *cis*-isomer has its acene rings centered over the hollow sites and follows the high-symmetry axis with the S atoms in atop positions of the Cu(111) surface. Conversely, for the *trans*-isomer, when the acene rings are centered over the hollow sites, the S atoms cannot be in the same registry with Cu(111) atoms

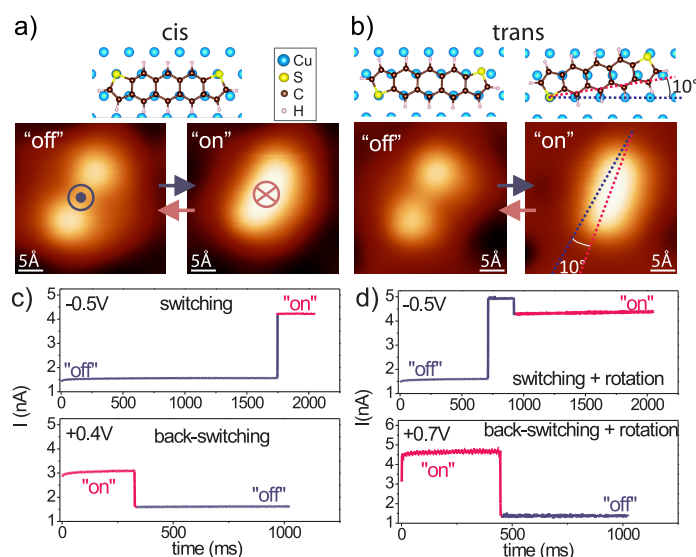


Figure 2. (a, b) STM images of the *cis*-ADT isomer and *trans*-ADT isomer and the top view of the ball-and-stick model representations on Cu(111), in the "off" and "on" conformation, respectively. Applying a negative bias pulse above the center of the molecules as indicated implies switching to the "on" conformation. The *trans*-ADT isomers rotate by about 10° during the switching process. (c, d) Current monitored as a function of time for the switching and back-switching process in an open-loop configuration. Before the feedback was turned off the tip was stabilized at 100 mV and 100 pA. Subsequently the tip was approached by 1 Å (and 0.8 Å for (d), lower panel, respectively) toward the molecule's center after turning off the feedback loop. Upper panel: Switching process of *cis*-ADT and *trans*-ADT isomers from the "off" state (lower conductance) to the "on" state (higher conductance), by applying a negative bias voltage. Lower panel: Back-switching from "on" to "off" conformation by applying a positive bias voltage.

of the surface. This suggests a reason why the *cis*-isomers do not change adsorption position while the *trans*-isomers rotate, as shown in panel (b). DFT calculations of the adsorption energy for both isomers and both conformations ("off" and "on" states) as a function of the tilt angle of the molecules with respect to the surface symmetry axis show minima at 0°. For the *trans*-isomer in the "on" state, there is only a small energy barrier to an adsorption conformation rotated by 10° (Supporting Information - Adsorption energy as function of tilt angle).

The detailed electronic density of states of the molecular conformations is summarized in Figure 3. Using an STM tip functionalized with an ADT molecule, the orbital structures of both conformations ("off" and "on") close to the Fermi level of the substrate (recorded at 5 mV) are resolved (Figure 3c,d). Comparing the images with the molecular orbitals calculated for the free molecule in the gas phase reveals that the states near E_F in the "off" state resemble the lowest unoccupied molecular orbital (LUMO), whereas in the "on" state they resemble the highest occupied molecular orbital (HOMO). This observation suggests that the switching between the two conformations is related to a charge transfer accompanied by a shift of the molecular orbitals. This behavior during the switching process, which is related to changes of the alignment of the energy levels, is obtained for both isomers. The only difference, as pointed out already, is the additional in-plane rotation in the case of the *trans*-ADT. Thus, the switching mechanism itself is similar for both isomers,

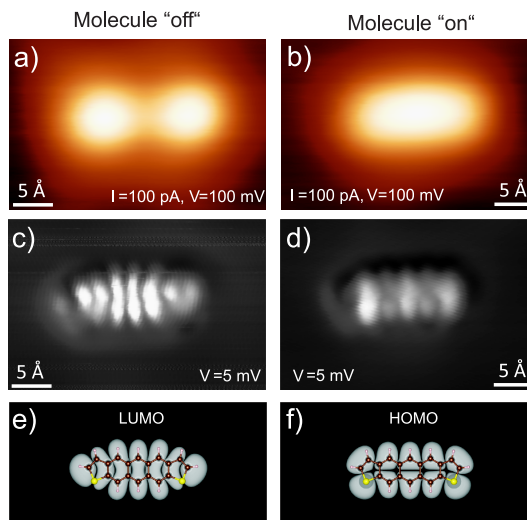


Figure 3. (a, b) STM topographic images of a *cis*-ADT molecule in the "off" and "on" conformation, respectively. (c, d) Constant height images resolving the orbital structures of the "off" and "on" conformation, resembling the LUMO and HOMO of a free molecule in the gas phase as shown in panels (e) and (f).

and for simplicity we will focus in the following on the *cis*-ADT.

To obtain a clear understanding of these two molecular conformations, DFT calculations of the electronic structure of the molecule–substrate system, varying the adsorption distance, were performed. As described below, the bent adsorption geometry of the ADT in the "off" state permits a closer adsorption distance,

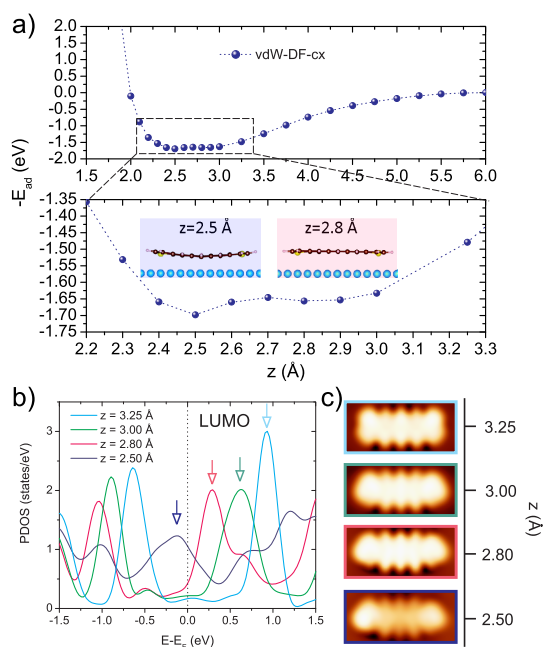


Figure 4. (a) Adsorption energy ($-E_{ad}$) of the *cis*-ADT isomer as a function of the adsorption height z on Cu(111) from vdW-DF-cx calculations. Lower panel: Close-up around the minima of the adsorption curve. Inset: Side view of the optimized geometries of the ADT molecule at the two adsorption heights $z = 2.5$ and 2.8 Å, where the two minima in $-E_{ad}$ appear, corresponding to the “off” and “on” conformations, respectively. (b) The PDOS calculated at the molecular adsorption distance of $z = 3.25$, 3.00 , 2.80 , and 2.50 Å highlights shifts of the LUMO decreasing the distance to the surface, as indicated by arrows. A partial filling of the LUMO orbital is obtained for the molecule in the “off” conformation at $z = 2.5$ Å. (c) Calculated molecular appearances at the corresponding distance above the surface. The geometry for adsorption distances of $z = 3$ and 3.25 Å is not fully optimized.

as compared to the planar case in the “on” state, which leads in the first case to a rather strong hybridization between the ADT molecule’s π -cloud and the Cu(111) metal surface, enough to compensate the Pauli repulsion and the energy penalty for the geometrical distortion. The calculations reveal two minima for the adsorption energies at $z = 2.5$ and 2.8 Å separated by a shallow energy barrier as shown in Figure 4a. These two minima appear after relaxing the (X,Y,Z) coordinates of the S atoms and the (X,Y) coordinates of the C and H atoms. The corresponding fully optimized molecular conformations with full relaxations of all atoms in (X,Y,Z) coordinates are indicated in the inset of Figure 4a.

In the molecular state at $z = 2.5$ Å, the “off” conformation, the molecule is adsorbed with the acene rings slightly closer to the surface compared to the S–Cu distance, which gives rise to the “dumbbell-like” appearance in the STM topographic images. This geometry corresponds to an adsorption state with a strong hybridization between the ADT molecule and the Cu(111) substrate that includes a significant amount of charge transfer to the LUMO of about one electron. By these means, the LUMO broadens and shifts to lower energies,

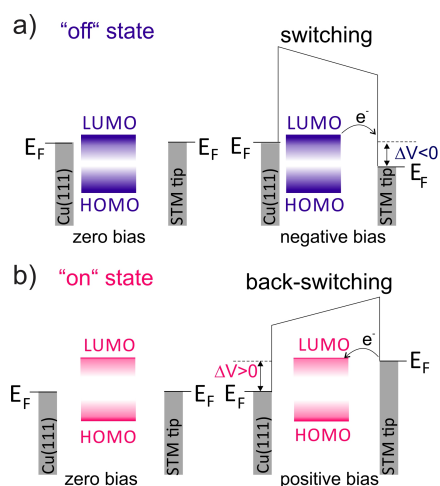


Figure 5. (a, b) Schematic representation of the energy level alignment for the molecule in both conformations showing a depopulation and population of the LUMO upon switching and back-switching, respectively.

thus closer to the Fermi energy, as visible in the projected density of states (PDOS) in Figure 4b. The “off” state is the ground state of the molecule, consistent with the experimental observation as discussed later.

In the “on” state the interaction between the ADT molecule and the Cu(111) substrate is weaker and corresponds to an adsorption state with a planar molecular geometry at larger distance of the acene rings from the surface. Here, no significant charge transfer between the surface and the molecule is present and the LUMO is essentially unoccupied, as shown in the calculated PDOS (Figure 4b). By increasing the distance between the molecule and the surface, the LUMO shifts further toward higher energies. In both the “on” and the “off” state, a hybridization between the ADT molecular orbitals and Cu(111) surface states exists. However, the dependence of the hybridization and the mixing of the HOMO–LUMO orbitals decreases by increasing the molecular adsorption distance. In the “off” state the LUMO shifts down to the Fermi energy, whereas in the “on” state, the LUMO is shifted to higher energies. The exact energy positions of the HOMO and LUMO molecular orbitals with respect to the metal states are difficult to accurately describe by DFT. The calculations still show a contribution of the LUMO at the Fermi level of the substrate even for an adsorption distance of $z = 2.8$ Å (Figure 4c). However, the shift of the LUMO to higher energies with the adsorption distance is well described, supporting the experimental findings. A schematic representation of the alignment of the energy levels, based on the calculated PDOS, in the two conformations and for both switching processes is depicted in Figure 5a,b.

In the “off” state, the ADT molecule is in a bent adsorption geometry with the acene rings close to the Cu(111) surface and the LUMO orbital partially occupied. By applying a negative bias voltage pulse

the LUMO is depopulated, destabilizing electronically the ADT, which facilitates the switching, *i.e.*, the switch to the “on” state with a planar geometry at larger distances. The reverse process, at positive bias voltage, is accompanied by a charge transfer into the LUMO, leading to the back-switching to the “off” state.

The switching and back-switching processes are induced at opposite polarities of the bias voltage, showing a characteristic hysteresis of the tunneling current while ramping the bias voltage; that is, it reflects a standard behavior of bipolar conductance switches (Figure 6a). The two step-like features in the current–voltage characteristic correspond to the switching and back-switching process. The threshold voltage and threshold current of the switching and back-switching processes are determined by measuring several hysteresis curves on top of different molecules and at different tip–sample distances and different sweeping times (from 10 s to maximum 50 s). In Figure 6b, the histogram of the bias voltages with both polarities is plotted, corresponding to switching into the “on” state and back into the “off” state. In Figure 6c, the distribution of the current values for both switching processes is represented. A broader range of voltage values is observed for the switching events at negative polarity, while for the back-switching at positive bias polarity, the distribution of current values is broader. This slightly different distribution range of voltages and currents for the switching and back-switching processes is related to different switching mechanisms attributed to the depopulation and population of the LUMO orbital. The bipolar switching process, where switching takes place at negative energies and back-switching at positive ones, is confined within an energy range of ± 0.6 V (for moderate tunnel parameters, *i.e.*, currents no larger than approximately 20 nA). Beyond that energy window, for instance at -0.8 V, current fluctuations associated with a toggling between the two states are observed. However, the switching mechanisms involved at those energies differ from those responsible for the bipolar switching. The current fluctuations show that the “off” state is energetically more favorable as the occupation time of the molecule in the “off” state is much higher compared to the occupation time of the molecule in the “on” state (Supporting Information - Analysis of switching behavior in time traces).

To confirm that the “on” conformation is the metastable state, we have tracked the duration of the “on” state of the *cis* molecules over time. Figure 7 shows the percentage of the *cis* molecules in the “on” state, which decreases exponentially in time with a decay time of about 7 h, after which the molecules are found in the “off” state. Similarly after deposition, all molecules are in the “off” state.

The switching and back-switching processes correspond to electronic transitions accompanied by

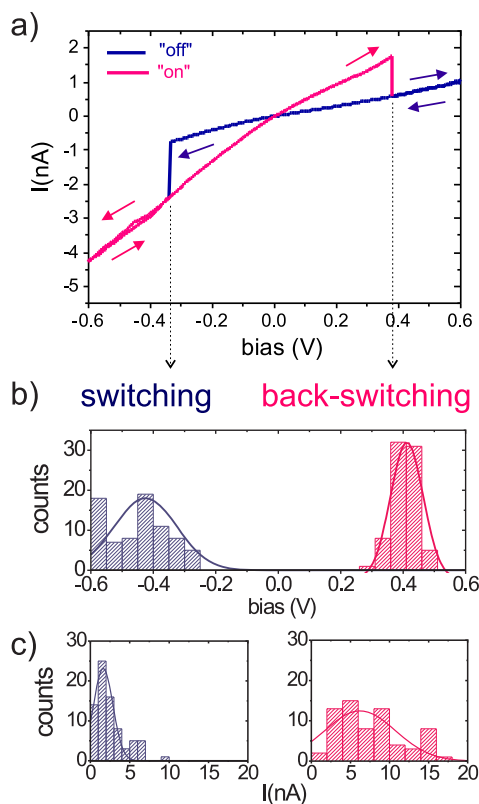


Figure 6. (a) Bipolar switching and back-switching hysteresis recorded by positioning the STM tip over the center of a *cis*-ADT isomer in the “off” conformation. The $I(V)$ curves were recorded as the bias voltage was ramped, with the feedback turned off, from 0.6 V to -0.6 V and back, as indicated by arrows in corresponding colors. The two step-like features in the current traces correspond to the switching and back-switching processes. (b) Bias voltage histograms with a bin of 50 mV corresponding to the switching (mean value -0.44 ± 0.1 V) and back-switching (mean value $+0.4 \pm 0.04$ V) processes, evaluated from several hysteresis curves taken above different molecules, at different tip–sample distances and with different sweeping times (from 10 s to maximum 50 s). (c) Current histograms of the switching (mean value 2.52 ± 1.88 nA) and back-switching (mean value 6.06 ± 3.68 nA) processes.

conformational changes between two different potential energy surfaces. These energy surfaces are defined by the Marcus parabolas of the corresponding diabatic states,³⁷ similar to the case of metal atoms adsorbed on a thin NaCl buffer layer grown on metal surfaces.³⁸ However, in our case the conformational changes occur at the molecular level of individual ADT molecules, which possess many degrees of freedom and, thus, allow for the existence of the two above-mentioned adsorption states: a bent geometry with the acene rings at closer distances, in which the optimal π -bonding length of the central acene rings compensates for the energy cost of the distortion imposed by the constraint of the S–Cu bond distance of the S-containing end groups, and a planar geometry at larger distances of the acene rings above the surface and optimal S–Cu bond distances. The optimal

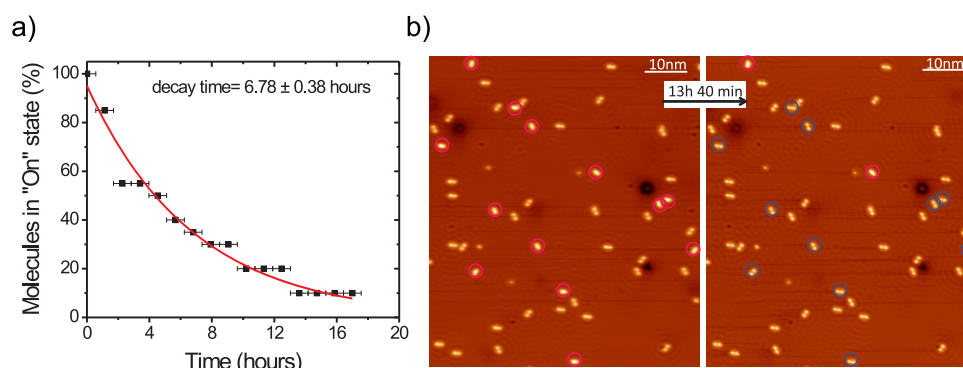


Figure 7. (a) Exponential decay time of the molecules from the “on” to the “off” state. (b) Corresponding STM images acquired in constant-current mode ($I = 40$ pA, $V = 50$ mV). Left panel: Several molecules have been switched to the “on” state. Right panel: The same area 13 h and 40 min later. Over time, the “on” molecules have switched spontaneously back to the “off” state.

adsorption distance between the central acene groups and the Cu(111) surface is very close to the pentacene–Cu(111) adsorption distance.^{33,34} However, the presence of S atoms in both end groups of the ADT molecule imposes an additional constraint due to the longer S–Cu bonding distance. The combination of both effects results in the two adsorption geometries, a bent geometry (“off” state) in which energy costs of the deformation are compensated by the optimal π -bonding of the acene groups to the metal surface, and a planar geometry (“on” state) without energy penalty for the geometrical distortion but with a longer bond length due to the S–Cu constraint. A similar behavior is described in the case of chlorinated benzene derivatives, as discussed in ref 29, but not in the case of pentacene. In this latter case there are no additional atoms, like the S atoms of ADT or the Cl atoms of benzene derivatives, introducing constraints to the optimal adsorption geometries.

Therefore, it is the molecular flexibility that allows the molecule to possess the two different bonding conformations to the metal surface, accompanied by changes of the molecular orbital occupations.

CONCLUSION

In conclusion, we have demonstrated reversible bipolar conductance switching of single ADT molecules adsorbed on Cu(111) and induced locally in a fully controlled manner in the STM tunneling junction. The comparison of the orbital resolved STM images with DFT calculations reveals that the switching process is accompanied by a geometric and an electronic change induced by charge transfer at the metal–organic interface associated with the depopulation and population of the LUMO orbital. These findings may be transferred to potential storage bits, allowing for controlled switching to “on” and “off” states at the individual molecular level.

EXPERIMENTAL AND COMPUTATIONAL METHODS

The experiments were performed under ultrahigh-vacuum conditions (UHV) with a home-built low-temperature scanning tunneling microscope (LT-STM) operating at a temperature of 6 K. The single Cu(111) crystal was prepared by repeated cycles of Ar^+ ion sputtering and subsequent annealing. A mixture of *cis*-antra[2,3-*b*:7,6-*b'*]dithiophene and *trans*-antra[2,3-*b*:6,7-*b'*]dithiophene isomers was sublimated with an organic molecular beam deposition technique on the Cu(111) surface with a sub-monolayer coverage. ADT molecules were purchased from Sigma-Aldrich. To prevent the molecules from reacting at the surface, the substrate is held at 200 K during deposition. Subsequently, the sample is transferred *in situ* to the LT-STM. Bias voltages are applied to the sample. The STM measurements were performed both in constant-current and constant-height modes.

The DFT-*vdW* calculations were done using the VASP code.^{39,40} The ADT/Cu(111) system was modeled using a 8×4 Cu(111) periodic supercell with four Cu layers; the ion–electron interaction was described with the projector augmented-wave (PAW) method,⁴¹ whereas the exchange and correlation potential was taken into account by the generalized gradient approximation (GGA)⁴² including the *vdW* dispersion forces using the *vdW*-DF-*cx* method.^{31,32} In the plane wave expansion we consider a kinetic energy cutoff of 500 eV. To satisfy the summations in the reciprocal space for the Brillouin zone, a mesh of 2×3 k points in the 1×1 unit cell was chosen. For all calculations the electronic

convergence criterion was 1×10^{-4} eV, while the convergence on forces in the relaxation was 0.05 eV/Å.

Conflict of Interest: The authors declare no competing financial interest.

Acknowledgment. We acknowledge funding by the Emmy-Noether-Program of the Deutsche Forschungsgemeinschaft, the SFB 767, and the Baden-Württemberg Stiftung. R.P. and A.A. thank the Basque Departamento de Universidades e Investigación (grant no. IT-756-13) and the Spanish Ministerio de Economía y Competitividad (grant no. FIS2013-48286-C2-8752-P) for financial support. R.P. and A.A. also acknowledge Joakim Löfgren and Per Hyldgaard for stimulating discussions about the *vdW*-DF-*cx* implementation.

Supporting Information Available: The Supporting Information is available free of charge on the ACS Publications website at DOI: 10.1021/acsnano.5b06000.

Additional details (PDF)

REFERENCES AND NOTES

1. Van der Molen, S. J.; Naaman, R.; Scheer, E.; Neaton, J. B.; Nitzan, A.; Natelson, D.; Tao, N.; Van der Zant, H.; Mayor, M.; Ruben, M.; *et al.* Visions for a Molecular Future. *Nat. Nanotechnol.* **2013**, *8*, 385–389.

- Kay, E. R.; Leigh, D. A.; Zerbetto, F. Synthetic Molecular Motors and Mechanical Machines. *Angew. Chem., Int. Ed.* **2007**, *46*, 72–191.
- Feringa, B. L.; Browne, W. R. *Molecular Switches*, 2nd ed.; Wiley-VCH: Weinheim, 2011; pp 1–792.
- Eigler, D. M.; Schweizer, E. K. Positioning Single Atoms with a Scanning Tunneling Microscope. *Nature* **1990**, *344*, 524–526.
- Iancu, V.; Hla, S.-W. Realization of a Four-Step Molecular Switch in Scanning Tunneling Microscope Manipulation of Single Chlorophyll Molecules. *Proc. Natl. Acad. Sci. U. S. A.* **2006**, *103*, 13718–13721.
- Wang, Y.; Kröger, J.; Berndt, R.; Hofer, W. A. Pushing and Pulling a Sn Ion through an Adsorbed Phthalocyanine Molecule. *J. Am. Chem. Soc.* **2009**, *131*, 3639–3643.
- Fu, Y.-S.; Schwöbel, J.; Hla, S.-W.; Dilullo, A.; Hoffmann, G.; Klyatskaya, S.; Ruben, M.; Wiesendanger, R. Reversible Chiral Switching of Bis(phthalocyaninato) Terbium(III) on a Metal Surface. *Nano Lett.* **2012**, *12*, 3931–3935.
- Ohmann, R.; Vitali, L.; Kern, K. Actuated Transitory Metal-Ligand Bond As Tunable Electromechanical Switch. *Nano Lett.* **2010**, *10*, 2995–3000.
- Albrecht, F.; Neu, M.; Quest, C.; Swart, I.; Repp, J. Formation and Characterization of a Molecule-Metal-Molecule Bridge in Real Space. *J. Am. Chem. Soc.* **2013**, *135*, 9200–9203.
- Mohn, F.; Repp, J.; Gross, L.; Meyer, G.; Dyer, M. S.; Persson, M. Reversible Bond Formation in a Gold-Atom-Organic-Molecule Complex as a Molecular Switch. *Phys. Rev. Lett.* **2010**, *105*, 266102.
- Leung, L.; Lim, T.; Polanyi, J. C.; Hofer, W. A. Molecular Calipers Control Atomic Separation at a Metal Surface. *Nano Lett.* **2011**, *11*, 4113–4117.
- Swart, I.; Sonleitner, T.; Repp, J. Charge State Control of Molecules Reveals Modification of the Tunneling Barrier with Intramolecular Contrast. *Nano Lett.* **2011**, *11*, 1580–1584.
- Walch, H.; Leoni, T.; Guillermet, O.; Langlais, V.; Scheuermann, A.; Bonvoisin, J.; Gauthier, S. Electromechanical Switching Behavior of Individual Molecular Complexes of Cu and Ni on NaCl-Covered Cu(111) and Ag(111). *Phys. Rev. B: Condens. Matter Mater. Phys.* **2012**, *86*, 075423.
- Fu, Y.-S.; Zhang, T.; Ji, S.-H.; Chen, X.; Ma, X.-C.; Jia, J.-F.; Xue, Q.-K. Identifying Charge States of Molecules with Spin-Flip Spectroscopy. *Phys. Rev. Lett.* **2009**, *103*, 257202.
- Leoni, T.; Guillermet, O.; Walch, H.; Langlais, V.; Scheuermann, A.; Bonvoisin, J.; Gauthier, S. Controlling the Charge State of a Single Redox Molecular Switch. *Phys. Rev. Lett.* **2011**, *106*, 216103.
- Uhlmann, C.; Swart, I.; Repp, J. Controlling the Orbital Sequence in Individual Cu-Phthalocyanine Molecules. *Nano Lett.* **2013**, *13*, 777–780.
- Riedel, D.; Bocquet, M.-L.; Lesnard, H.; Lastapis, M.; Lorente, N.; Sonnet, P.; Dujardin, G. Selective Scanning Tunneling Microscope Electron-Induced Reactions of Single Biphenyl Molecules on a Si(100) Surface. *J. Am. Chem. Soc.* **2009**, *131*, 7344–7352.
- Liljeroth, P.; Repp, J.; Meyer, G. Current-Induced Hydrogen Tautomerization and Conductance Switching of Naphthalocyanine Molecules. *Science* **2007**, *317*, 1203–1206.
- Henzl, J.; Mehlhorn, M.; Gawronski, H.; Rieder, K.-H.; Morgenstern, K. Reversible Cis-Trans Isomerization of a Single Azobenzene Molecule. *Angew. Chem., Int. Ed.* **2006**, *45*, 603–606.
- Morgenstern, K. Isomerization Reactions on Single Adsorbed Molecules. *Acc. Chem. Res.* **2009**, *42*, 213–223.
- Kumagai, T.; Hanke, F.; Gawinkowski, S.; Sharp, J.; Kotsis, K.; Waluk, J.; Persson, M.; Grill, L. Thermally and Vibrationally Induced Tautomerization of Single Porphycene Molecules on a Cu(110) Surface. *Phys. Rev. Lett.* **2013**, *111*, 246101.
- Simpson, G. J.; Hogan, S. W. L.; Caffio, M.; Adams, C. J.; Früchtl, H.; van Mourik, T.; Schaub, R. New Class of Metal Bound Molecular Switches Involving H-Tautomerism. *Nano Lett.* **2014**, *14*, 634–639.
- Parschau, M.; Passerone, D.; Rieder, K.-H.; Hug, H. J.; Ernst, K.-H. Switching the Chirality of Single Adsorbate Complexes. *Angew. Chem., Int. Ed.* **2009**, *48*, 4065–4068.
- Aleman, M.; Peters, M. V.; Hecht, S.; Rieder, K.-H.; Moresco, F.; Grill, L. Electric Field-Induced Isomerization of Azobenzene by STM. *J. Am. Chem. Soc.* **2006**, *128*, 14446–14447.
- Serrate, D.; Moro-Lagares, M.; Piantek, M.; Pascual, J. I.; Ibarra, M. R. Enhanced Hydrogen Dissociation by Individual Co Atoms Supported on Ag(111). *J. Phys. Chem. C* **2014**, *118*, 5827–5832.
- Qiu, X. H.; Nazin, G. V.; Ho, W. Mechanisms of Reversible Conformational Transitions in a Single Molecule. *Phys. Rev. Lett.* **2004**, *93*, 196806.
- Wu, S. W.; Ogawa, N.; Ho, W. Atomic-Scale Coupling of Photons to Single-Molecule Junctions. *Science* **2006**, *312*, 1362–1365.
- Lee, J.; Tallarida, N.; Rios, L.; Perdue, S. M.; Apkarian, V. A. Single Electron Bipolar Conductance Switch Driven by the Molecular Aharonov-Bohm Effect. *ACS Nano* **2014**, *8*, 6382–6389.
- Liu, W.; Filimonov, S. N.; Carrasco, J.; Tkatchenko, A. Molecular Switches from Benzene Derivatives Adsorbed on Metal Surfaces. *Nat. Commun.* **2013**, *4*, 3569.
- Anthony, J. E. Functionalized Acenes and Heteroacenes for Organic Electronics. *Chem. Rev.* **2006**, *106*, 5028–5048.
- Berland, K.; Hylgaard, P. Exchange Functional that Tests the Robustness of the Plasmon Description of the Van der Waals Density Functionals. *Phys. Rev. B: Condens. Matter Mater. Phys.* **2014**, *89*, 035412-1–035412-8.
- Björkman, T. Testing Several Recent van der Waals Density Functionals for Layered Structures. *J. Chem. Phys.* **2014**, *141*, 074708-1–074708-6.
- Toyoda, K.; Nakano, Y.; Hamada, I.; Lee, K.; Yanagisawa, S.; Morikawa, Y. First-Principles Study of the Pentacene/Cu(111) Interface: Adsorption States and Vacuum Level Shifts. *J. Electron Spectrosc. Relat. Phenom.* **2009**, *174*, 78–84.
- Koch, N.; Gerlach, A.; Duhm, S.; Glowatzki, H.; Heimel, G.; Vollmer, A.; Sakamoto, Y.; Suzuki, T.; Zegenhagen, J.; Rabe, J. P.; *et al.* Adsorption-Induced Intramolecular Dipole: Correlating Molecular Conformation and Interface Electronic Structure. *J. Am. Chem. Soc.* **2008**, *130*, 7300–7304.
- Lagoute, J.; Kanisawa, K.; Fölsch, S. Manipulation and Adsorption-Site Mapping of Single Pentacene Molecules on Cu(111). *Phys. Rev. B: Condens. Matter Mater. Phys.* **2004**, *70*, 245415.
- Milligan, P.; McNamara, J.; Murphy, B.; Cowie, B.; Lennon, D.; Kadodwala, M. A NIXSW and NEXAFS Investigation of Thiophene on Cu(111). *Surf. Sci.* **1998**, *412–413*, 166–173.
- Marcus, R. A. Electron Transfer Reactions in Chemistry. Theory and Experiment. *Rev. Mod. Phys.* **1993**, *65*, 599–610.
- Olsson, F. E.; Paavilainen, S.; Persson, M.; Repp, J.; Meyer, G. Multiple Charge States of Ag Atoms on Ultrathin NaCl Films. *Phys. Rev. Lett.* **2007**, *98*, 176803.
- Kresse, G.; Hafner, J. Ab Initio Molecular-Dynamics Simulation of the Liquid-Metal-Amorphous-Semiconductor Transition in Germanium. *Phys. Rev. B: Condens. Matter Mater. Phys.* **1994**, *49*, 14251–14269.
- Kresse, G.; Furthmüller, J. Efficient Iterative Schemes for Ab Initio Total-Energy Calculations Using a Plane-Wave Basis Set. *Phys. Rev. B: Condens. Matter Mater. Phys.* **1996**, *54*, 11169–1118.
- Blöchl, P. E. Projector Augmented-Wave Method. *Phys. Rev. B: Condens. Matter Mater. Phys.* **1994**, *50*, 17953–17979.
- Perdew, J. P.; Burke, K.; Ernzerhof, M. Generalized Gradient Approximation Made Simple [Phys. Rev. Lett. **77**, 3865 (1996)]. *Phys. Rev. Lett.* **1997**, *78*, 1396–1396.